

# Förster resonance energy transfer in a nanoscopic system on a dielectric interface

Subrata Batabyal, Tanumoy Mondol, Kaustuv Das and Samir Kumar Pal

Unit for Nano-science and Technology, S. N. Bose National Centre for Basic Sciences, Block JD, Sector III, Salt Lake, Kolkata 700098, India

E-mail: [skpal@bose.res.in](mailto:skpal@bose.res.in)

Received 26 July 2012, in final form 1 October 2012

Published 13 November 2012

Online at [stacks.iop.org/Nano/23/495402](http://stacks.iop.org/Nano/23/495402)

## Abstract

We investigate picosecond-resolved energy transfer between a quantum dot (donor) and an organic molecule (acceptor) in the proximity of a reflecting metallic/non-metallic surface. We demonstrate experimentally that the Förster resonance energy transfer (FRET) is significantly influenced by the proximity of the mirror. Locating a cadmium selenide quantum dot (donor: D) attached to an organic dye merocyanine (acceptor: A) at well-defined positions from the reflecting silver/silicon surface allows the transfer rate to be determined as a function of distance from the surface. An attempt to fit the experimental data to a model relying upon the change of the apparent energy transfer rate due to interference of direct and reflected light waves reveals reasonably good results. The results show that the observed FRET rate in a D–A pair on the mirror surface is oscillating in nature, providing information for the measured energy transfer, which could be potentially different from that of the actual transfer due to optical interference.

## 1. Introduction

The efficiency of a photon source is heavily dependent on its immediate environment [1–4]. A precise control over the excited state lifetime and emission quantum yield of organic dyes and inorganic quantum dots (QDs) involving fundamental physics of light-matter interactions is important to a number of branches of science [5–7]. Energy migration from a photon source through resonant dipole–dipole interaction (RDDI) is found to be an important way to control the emission property of the sample [8, 9]. The most important natural example of the utilization of RDDI is photosynthesis [10]. The process is of increasing importance as a means of improving functionality and efficiency of organic material based LED [11] and laser devices [10, 12]. For a practical use of a photon source under RDDI (an energy donor (D) in the proximity of an acceptor (A)) several situations can be considered. The D–A pair may be confined in a microcavity [8, 13]. It has been demonstrated that the Förster resonance energy transfer (FRET) in the D–A pair is heavily influenced by the photonic mode density [8]. By

locating D and A molecules at well-defined positions, [8] the study shows the transfer rate to be determined as a function of both mutual separation and cavity length. Sometimes the proximity of highly conducting noble metals (Ag, Au) to the D/A molecules may lead to an extra channel for the deactivation of the D molecules through photon–surface plasmon interaction [14, 15]. In a recent study [16], we have shown that the non-radiative energy transfer from the emitting semiconductor QDs to the plasmonically active silver surface is FRET type rather than the well known nano-surface energy transfer (NSET) type.

The proximity of the D–A pair beyond the distance ( $d > \lambda/10$ ) of the plasmonic interaction from the metal surface may not arise in some cases. In that case, the following two situations may arise. Firstly, if the D–A pair is within a distance of 25 nm from the metal surface, the D–A may be considered to be in a half optical cavity [8]. In that case, FRET is expected to be affected by the local density of the photonic mode (PMD). Secondly, if the location of the D–A pair is beyond 100 nm from the metallic reflective surface, there would be a negligible effect of either PMD or plasmonic

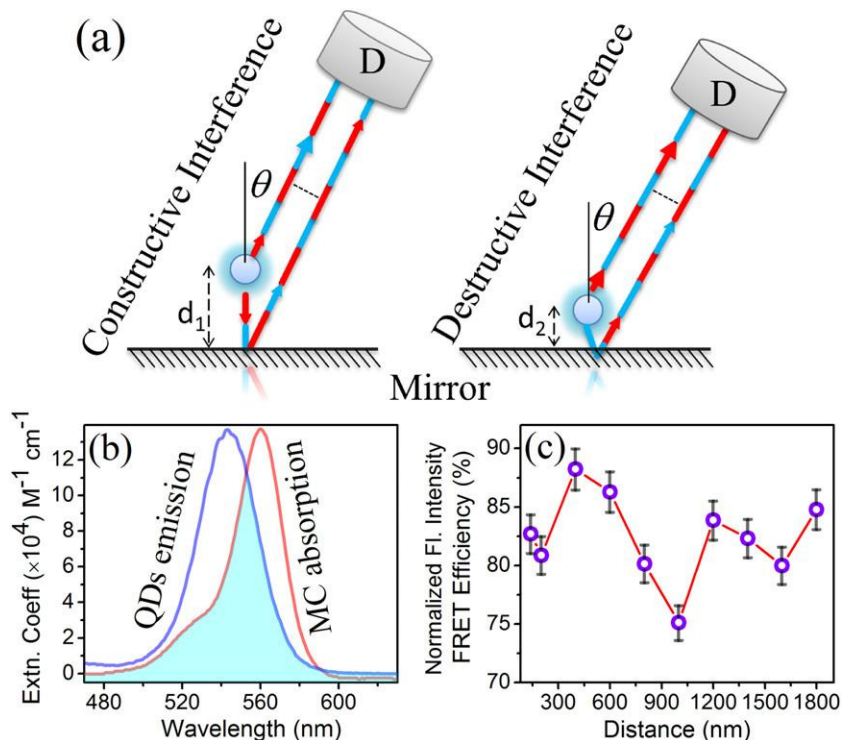


**Figure 1.** (a) Schematic for the optical interference near the interfaces. The constructive (for  $d_1$ ) and destructive (for  $d_2$ ) interference is shown for a dipole emitter near the reflective mirror. (b) Spectroscopic data for the donor (QDs) and acceptor (merocyanine: MC) molecules. The shaded region depicts the overlap between QD emission and the MC absorption cross-section. The donor emission is normalized with respect to the MC extinction coefficient. The overlap integral is estimated to be  $5.5 \times 10^{15} M^{-1} cm^{-1} nm^4$  considering the extinction coefficient of MC ( $138\,000 M^{-1} cm^{-1}$ ) at 560 nm. (c) Change in apparent FRET efficiency for the conjugate dipolar system, QDs–MC, due to the optical interference.

interaction on the rate of FRET. Here, we demonstrate that the apparent rate of FRET is significantly affected by studying picosecond-resolved transfer of excitation energy between QDs and an organic dye at a distance of  $d > 100$  nm from the metallic surface (figure 1(c)).

The physical mechanism of FRET depends on the D–A separation,  $R$ . When D and A are very close, a virtual photon initiates the non-radiative energy transfer process and the pre-requirement for FRET is achieved. On the other hand, when D and A are far apart ( $R > \lambda/10$ ), the energy transfer follows radiative pathways, D–A coupling being mediated by a real photon [8, 17]. It has to be noted that dipole–dipole interaction plays a central role in both the above two processes, the radiative process relies on a dipole far field while non-radiative transfer proceeds through the evanescent near field components. The efficiency of FRET from the excited state donor (D) to the nearby acceptor (A) is expressed as [17],

$$E = \frac{R_0^6}{R_0^6 + R^6}. \quad (1)$$

The characteristic Förster distance  $R_0$  is defined by [17],

$$R_0 = 0.211 \times [\kappa^2 n^{-4} \Phi_D J(\lambda)]^{1/6} \quad (\text{in } \text{Å}) \quad (2)$$

where  $\kappa^2$ , the orientation factor, is taken to be 0.66 for random D–A orientation and the value of  $n$  (refractive index of the

medium) is supposed to be 1.4.  $\Phi_D$  refers to the quantum yield of the donor system in the absence of an acceptor. The overlap integral  $J(\lambda)$  expresses the degree of spectral overlap between the donor emission and the acceptor absorption.

In an earlier study, it has been shown that the emission of the radiation for an excited molecule (atom) in front of a mirror is significantly influenced [18]. By studying the fluorescence lifetime of europium-dibenzoylmethene complex, at various well-defined distances from a silver mirror, the study has concluded that the change in the fluorescence lifetime of the dye complex in the interface between two dielectrics of different refractive indices, is solely a consequence of optical interference between two waves (reflected and non-reflected) as shown in figure 1. Similar studies have also been recently carried out [19–22]. The radiation of an oscillating electric dipole in front of a mirror and the consequence of the optical interference is shown in figure 1, where the radiation essentially depends on the angle of detection ( $\theta$ ) as well as the separating distance ( $d$ ) between emitter and surface. When the path difference between the direct and reflected beam is such that constructive interference occurs, the molecule will radiate strongly in the direction of observation [18]. As a consequence, amplification by the interface dipole radiation, is twice the power as without the mirror ( $\tau_m = 1/2\tau$ ), where  $\tau_m$  and  $\tau$  are the fluorescence lifetimes of the molecule in the presence and absence of the mirror respectively. In contrast, when the path difference is

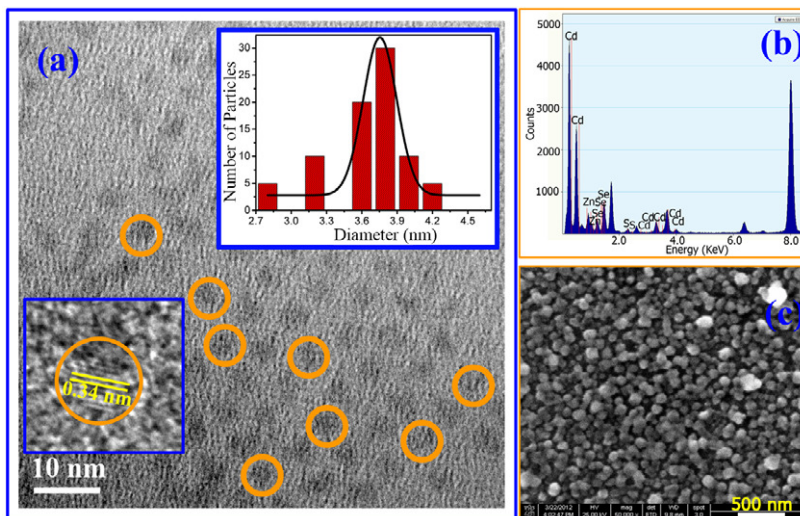


**Figure 2.** (a) TEM images of the CdSe/ZnS QDs. The size distributions of the particles are represented in the inset figure. The particle diameter was estimated to be 3.8 nm. The inset snapshot represents the HRTEM of the particle with distinct crystal fringes. (b) EDAX analysis of the QDs revealing the atomic compositions. (c) The SEM image of the silver film over the glass substrate.

half a wavelength smaller so that the direct and reflected beam interferes destructively, quenching of radiation occurs where the dipole cannot radiate revealing  $\tau_m = \infty$ . As the energy donor–acceptor pair (D–A) is considered as a coupled oscillating dipole [23], the efficiency of the energy transfer between a FRET pair in front of a mirror is of importance as a means of understanding optical radiation from the optical devices. The absence of appropriate experimental information so far leaves open the question as to whether apparent FRET efficiency can be changed by the proximity of a reflecting surface and this is the motive for the present work. An experiment consisting of quantifying the quenching by a FRET acceptor as a function of the distance of the D–A pair from reflective surfaces is illustrated in our present study.

## 2. Experimental details

In our experiment, trioctylphosphine oxide (TOPO)-capped core shell CdSe/ZnS QDs in toluene (Catskill Green) with a photoluminescence (PL) peak at 542 nm were obtained from Evident Technologies, Inc. (New York). Merocyanine-540: MC (1,3-dibutyl-5-[4-[3-(3-sulfopropyl)-2-benzoxazolinyldiene]-2,4-butyldiene]-2 thiobarbituric acid sodium salt), poly vinyl alcohol (PVA) and toluene were obtained from Sigma. The characterization of the QDs was done using a transmission electron microscope (TEM). The average diameter of the QDs obtained from the TEM image was estimated to be 3.8 nm and the TEM image is represented in figure 2(a). The inset figure represents the size distribution of the QDs. The inset snapshot reveals the existence of a fringe ensuring high crystallinity of the QDs. The interplanar distance of 0.34 nm is consistent with the (111) planes of cubic CdSe [24]. Energy dispersive x-ray spectroscopy (EDAX) analysis of the QDs provided the atomic composition of the QDs as represented in figure 2(b). The reflective silver film was prepared on a glass substrate by chemical reduction of silver nitrate by sodium hydroxide in the presence of

sugar and ammonium hydroxide. For the preparation of the silver mirror, the chemicals used were obtained from Sigma. The silver film was characterized under a scanning electron microscope (SEM) as shown in figure 2(c).

One side polished silicon wafer, purchased from Semiconductor Wafer Inc., was used as a model reflecting non-metallic surface. The distance variation was done using PVA spacer layers of different thickness produced by the spin-coating technique. The thickness of the PVA layer was varied from 0.1 to 2.4  $\mu\text{m}$ . QDs–MC conjugate was prepared by overnight stirring of the QDs with MC in toluene followed by sonication and filtration to remove any undissolved MC in the solution. Because of the high affinity of ZnS to the sulfur compared to oxygen, on mixing CdSe/ZnS QDs with MC, the TOPO ligands around the QDs were replaced by MC due to the presence of sulfur atoms in it. Thus a surface-attached coupled dipole pair (D–A) is formed. Finally, the QDs–MC conjugate was spin cast on PVA-coated Ag film/Si wafers and the PL lifetimes of the samples were measured using Life-spec Spectrometer (Edinburgh Instruments, UK). All spectroscopic measurements were performed at room temperature. The excitation at 375 nm (IRF = 70 ps) was obtained using a pulsed laser diode. The excitation was vertically polarized, and the emission was recorded through a polarizer oriented at 55° from the vertical position. The front surface emission was collected at a fixed angle of the detector at 45°. A long-pass filter at 420 nm was used in the collection path to effectively eliminate the possible scattered excitation. The PL decay transients were fitted to a multi-exponential functional form with a nonlinear least squares fitting routine, which allowed the average lifetime ( $\tau_{\text{avg}} = \sum_{i=1}^n A_i \tau_i$  where  $\sum_{i=1}^n A_i = 1$ ) to be calculated from a weighted average of the lifetime components [17, 25]. In our experiment, the fluorescence transients were fitted to a tri-exponential decay function to obtain the best fitting of the experimental data. The average lifetimes of the various systems under study are summarized in table 1.

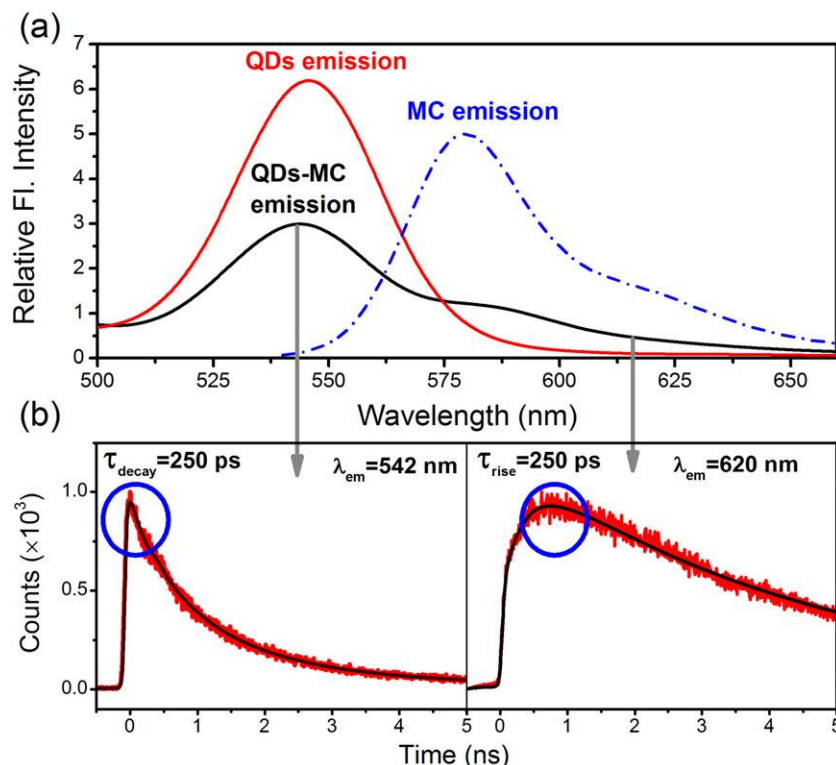


**Figure 3.** (a) Steady-state spectrum of QDs in the presence and absence of MC is shown. The PL of QDs in the presence of MC is significantly quenched. Alongside, the emission spectrum of MC is shown (dotted lines). From the figure, it is evident that at 542 nm detection wavelength, the possible contribution of MC emission can be safely ruled out. (b) Represents the PL decay of QDs–MC conjugate systems collected at two different wavelengths, 542 and 620 nm. The decay collected at 542 nm shows the lifetime quenching of QDs due to energy transfer from QDs to MC and is reflected by the faster decay component of 250 ps. The decay collected at 620 nm exhibits the lifetime of MC and, due to energy transfer, the rise component of 250 ps is manifested in its lifetime decay.

**Table 1.** Average fluorescence lifetime (ns) for QDs and QDs–MC conjugate on silver and silicon surface.

Silver			Silicon		
Distance (nm)	$\tau_{\text{QDs}}$	$\tau_{\text{QDs-MC}}$	Distance (nm)	$\tau_{\text{QDs}}$	$\tau_{\text{QDs-MC}}$
100	7.51	0.62	200	7.43	0.55
200	7.45	0.81	350	9.14	0.61
350	7.38	0.75	600	9.04	0.63
500	6.86	0.82	900	8.15	0.60
800	7.79	0.70	1200	7.67	0.59
1100	7.02	1.06	1500	7.36	0.58
1400	7.09	0.78	1800	8.62	0.78
1600	6.90	0.72	2100	8.85	0.62
			2300	7.85	0.61

### 3. Results and discussion

Steady-state emission quenching of QDs in the presence of MC is represented in figure 3(a). Alongside, the emission spectrum of MC is also shown. As shown in the figure, the possible contribution of MC emission at 542 nm can be safely ruled out. Figure 3(b) represents the PL lifetime of the QDs–MC complex collected at 542 and 620 nm. The efficiency of the energy transfer from QDs to MC is justifiable from the decay component in the QDs lifetime (542 nm) which is manifested in the rise component in the MC (620 nm) lifetime. It has to be noted that both the lifetime and steady-state quenching of QDs in the QDs–MC

conjugate occur due to non-radiative energy transfer from QDs to MC and not due to surface modification of QDs by the MC ligand [26]. To highlight the significant role played by the silver interface, we measured the PL lifetime of both point dipoles (QDs) and the coupled dipole system (QDs–MC conjugate) as a function of distance between them and the silver interface for several different spacer layers. If the presence of the interface was of no consequence, one would expect the lifetime in the presence and absence of the interface to be unaffected. However, for both the point dipole and coupled dipole system (D–A), significant lifetime variation was observed, which is graphically presented in figure 4. Figure 4(a) represents the time-resolved PL decay



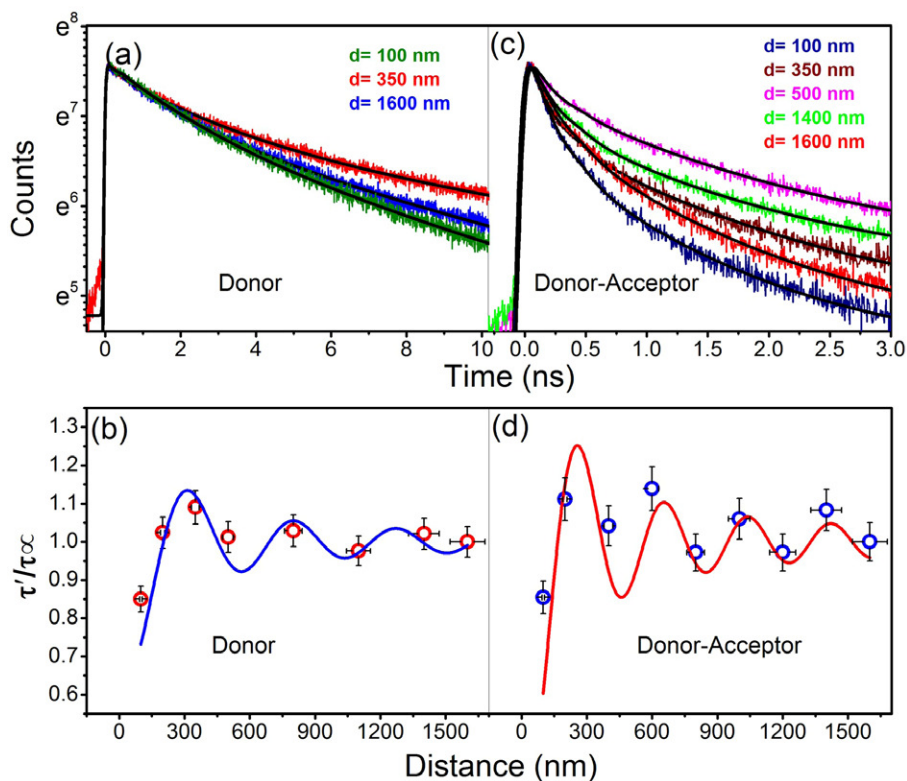


**Figure 4.** (a) and (c) The fluorescence transients of QDs and QDs–MC conjugate with varying distance from the silver mirror. The excitation wavelength was 375 nm. The decay was collected at the emission maximum of QDs (542 nm). (b) and (d) The dependences of QD lifetime on mirror distances are graphically presented. The open circles with 5% error bar represent the experimental data. The line curve is the fitted plot of the experimental data to equation (5).

of CdSe/ZnS QDs located at various distances from the silver interface. The distance was varied up to *about* 1.6  $\mu\text{m}$ . The PL decays show the enhancement and quenching of lifetime depending on the spacer layer thickness. The relative lifetime variation is plotted against the distance in figure 4(b). As shown in the figure, the lifetime follows oscillatory behaviour. The D–A distance from the time-resolved FRET on bare glass was estimated to be 3.7 nm which is consistent with our system under study (1.9 nm CdSe core + 0.3 nm ZnS shell + 1.2 nm ligand distance). On the silver surface, the lifetime of QDs is significantly quenched, which is due to the energy transfer from QDs to silver film, and is consistent with one of our previous studies [16]. However, in the presence of the PVA spacer layer, there is no direct energy transfer feasibility from QDs to silver film due to the larger distance ( $d > 100$  nm). Therefore, the lifetime variation of QDs is solely due to the light wave interference. In the next step, we measured the PL lifetime of the QDs–MC conjugate, a dipole pair, which serves as a FRET pair. The lifetime decays of the QDs–MC conjugate being at various distances from the interface are presented in figure 4(c) and the oscillatory nature of the relative lifetime values are plotted in figure 4(d). The outcome of this lifetime variation greatly influences the apparent energy transfer efficiency as presented in figure 1(c). The apparent energy transfer efficiency, estimated considering the lifetime changes for both the donor (QDs) and donor–acceptor (QDs–MC) system at various spacer distances due to optical interference, changes

from 75% to 89%. In order to establish the fact that the lifetime alteration is solely due to reflective interference, we further extended our study using a silicon wafer as a reflective interface. The polished silicon wafer does not possess any plasmonic absorption characteristic like the silver film [27]. For the silicon wafer, results similar to those for the silver surface were obtained (figure 5). The fluorescence lifetime of the coupled dipolar system was also found to have distance dependency. The study with silicon clearly rules out the possibility of direct energy transfer that might arise due to the silver absorptivity. It is now instructive to compare the obtained data with the existing model. The lifetime variation in front of the reflecting surface as described by Drexhage [18] is relevant to our system under study. In the case of a plane reflective surface, the decay time ( $\tau$ ) can be expressed as follows.

In the case of an electric dipole oscillator parallel to the mirror,

$$\frac{\tau}{\tau_{\infty}} = \left[ 1 + \frac{3}{4} \int_0^1 \rho_{\parallel}(u) u^2 \cos(xu - \delta_{\parallel}(u)) du + \frac{3}{4} \int_0^1 \rho_{\perp}(u) u^2 \cos(xu - \delta_{\perp}(u)) du \right]^{-1} \quad (3)$$

where  $x = \frac{4\pi n d}{\lambda}$ ,  $u = \cos \theta$ ,  $\rho_{\parallel}(u)$ ,  $\rho_{\perp}(u)$  are reflection coefficients,  $\delta$  is the phase shift and  $n$  is the refractive index of the medium in front of the surface. In the case of a perfect

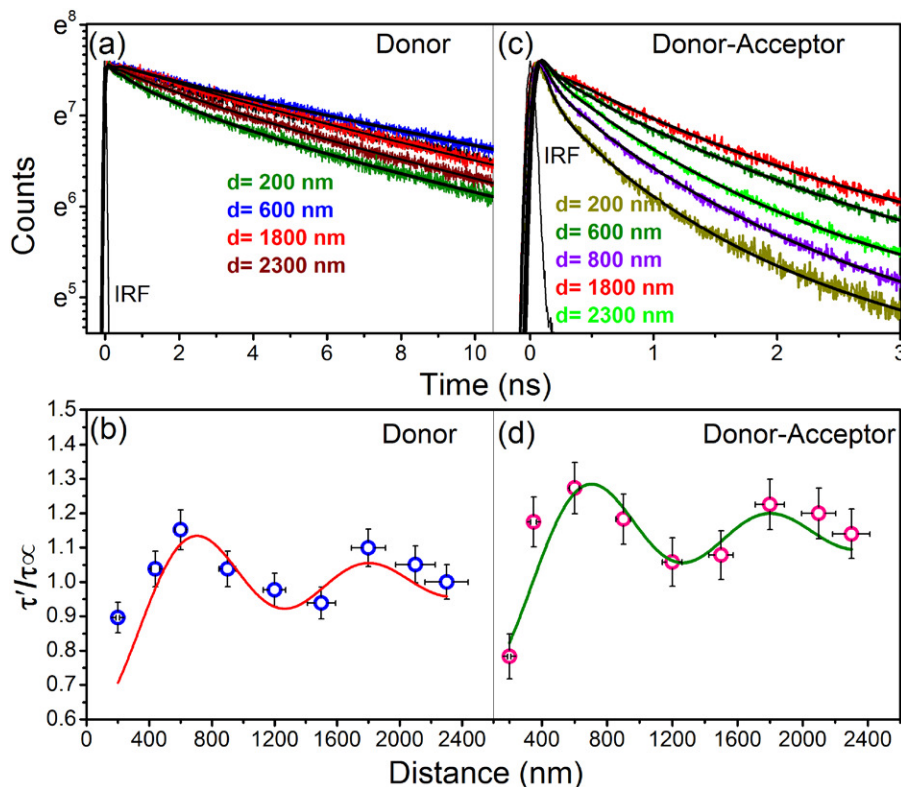


**Figure 5.** (a) and (c) The fluorescence transients of QDs and QDs–MC conjugate with varying distance from the silicon surface. The excitation wavelength was 375 nm. The decay was collected at the emission maximum of QDs (542 nm). (b) and (d) The dependences of QD lifetime on mirror distances are graphically presented. The open circles with 3% error bar represent the experimental data. The line curve is the fitted plot of the experimental data to equation (5).

mirror, the above equation can be solved, and the equation becomes:

$$\frac{\tau}{\tau_{\infty}} = \left[ 1 - \frac{3 \sin x}{2x} - \frac{3 \cos x}{2x^2} + \frac{3 \sin x}{2x^3} \right]^{-1}. \quad (4)$$

If one considers the radiation-less deactivation to be affected by the mirror, then the true decay time would be  $\tau'$  and the above equation can be rearranged as follows:

$$\frac{\tau'}{\tau_{\infty}} = \left[ \frac{1}{1 + \eta_{\infty} \left( \frac{\tau_{\infty}}{\tau} \right)} \right] \quad (5)$$

where  $\eta_{\infty}$  is the quantum yield of the emitting state. We applied the above theoretical model and found reasonably good fitting of our experimental data to equation (5). The fitting curves are represented along the respective figures (figures 4 and 5). The obtained quantum efficiencies (0.3–0.5) from the theoretical fitting are reasonably good when compared with the actual quantum yield of the donor system QDs (*namely* 0.4). The quantum efficiency of the donor system (D) obtained by the model fit reflects the intrinsic quantum yield of the donor (QDs), even for the D–A conjugate system. An attempt to fit the experimental data by considering the perpendicular orientation of the dipole to the mirror surface, for both the D and D–A systems, was found not to be appropriate for our systems. As described in equation (3), the decay time of the emitter depends on emission wavelength, reflection coefficient, phase shift and also the refractive index

of the medium in front of the mirror. The reflectivity and phase shifts for both the materials (silver and silicon) would be different, which will eventually contribute to the oscillatory nature of the dipolar emission.

#### 4. Conclusion

In summary, this new understanding can be put to practical use. The theoretical model fit for a conjugate dipolar system having lifetime dependency on surface–dipole separation ( $d$ ) could provide useful information about the intrinsic quantum efficiency of the emitting dipole, which is otherwise not obtainable by the general approach of quantum efficiency estimation using the standard steady state and time-resolved technique. The practical application of such understanding includes many optical devices, and one of the prominent examples is in organic material based light-emitting diodes (OLEDs). In an OLED, within a microcavity, interference effects can significantly alter both the intensity and the spectrum of the emitted light [28]. In the case of organic LEDs, the microcavity plays a vital role where the organic layers remain sandwiched between two parallel reflectors [29, 30]. Usually, in a state-of-the-art OLED, one of the reflectors is a metallic mirror while the other is a Bragg reflector. The light beam interferes multiple times between the two reflectors producing enhanced forward-emission and spectral narrowing in these devices. An ordinary OLED, however,

consists of only one effective reflector, a metallic cathode. In this geometry, wide-angle interference is anticipated to dominate when directly radiated and reflected waves overlap with each other. The thickness of the light-emitting layer controls the optical path difference between the direct and the reflected waves and is crucial to the overall efficiency including the angular intensity distribution and operational frequency bandwidth of an OLED.

## Acknowledgments

SB thanks CSIR, India for the research fellowship. We thank DST for financial grants SR/SO/BB-15/2007.

## References

- [1] Anger P, Bharadwaj P and Novotny L 2006 *Phys. Rev. Lett.* **96** 113002
- [2] Kleppner D 1981 *Phys. Rev. Lett.* **47** 233
- [3] Worthing P T, Amos R M and Barnes W L 1999 *Phys. Rev. A* **59** 865
- [4] Chance R R, Prock A and Silbey R 1978 *Adv. Chem. Phys.* **37** 1
- [5] Leistikow M D, Johansen J, Kettelarij A J, Lodahl P and Vos W L 2009 *Phys. Rev. B* **79** 045301
- [6] Akahane Y, Asano T, Song B S and Noda S 2003 *Nature* **425** 944
- [7] Wolfgang C S, Masayuki F, Makoto Y, Takashi A and Susumu N 2007 *Appl. Phys. Lett.* **90** 231101
- [8] Andrew P and Barnes W L 2000 *Science* **290** 785
- [9] Sadeghi S M, West R G and Nejat A 2011 *Nanotechnology* **22** 405202
- [10] Baldo M A, Thompson M E and Forrest S R 2000 *Nature* **403** 750
- [11] Coe S, Woo W, Bawendi M and Bulović V 2002 *Nature* **420** 800
- [12] Dodabalapur A, Rothberg L J, Jordan R H, Miller T M, Slusher R E and Phillips J M 1996 *J. Appl. Phys.* **80** 6954
- [13] Wang X Y, Shih C K, Xu J F and Xiao M 2006 *Appl. Phys. Lett.* **89** 113114
- [14] Andrew P and Barnes W L 2004 *Science* **306** 1002
- [15] Bellessa J, Bonnand C, Plenet J C and Mugnier J 2004 *Phys. Rev. Lett.* **93** 036404
- [16] Batabyal S, Makhil A, Das K, Raychaudhuri A K and Pal S K 2011 *Nanotechnology* **22** 195704
- [17] Lakowicz J R 2006 *Principles of Fluorescence Spectroscopy* (New York: Kluwer Academic/Plenum)
- [18] Drexhage K H 1970 *J. Lumin.* **1–2** 693
- [19] Achermann M 2010 *J. Phys. Chem. Lett.* **1** 2837
- [20] Bradshaw D S, Peck J N T, Oganessian V S and Andrews D L 2010 *J. Phys. Chem. Lett.* **1** 2705
- [21] Zhang J Y, Wang X Y and Xiao M 2002 *Opt. Lett.* **27** 1253
- [22] Zhang Y, Komarala V K, Rodriguez C and Xiao M 2008 *Phys. Rev. B* **78** 241301
- [23] Hofkens J *et al* 2003 *Proc. Natl Acad. Sci. USA* **100** 13146
- [24] Rong H and Hongchen G 2006 *Colloids Surf.* **272** 111
- [25] Periasamy N 1988 *Biophys. J.* **54** 961
- [26] Narayanan S S and Pal S K 2006 *J. Phys. Chem. B* **110** 24403
- [27] Nagpal P, Lindquist N C, Oh S -H and Norris D J 2009 *Science* **325** 594
- [28] So S K, Choi W K, Leung L M and Neyts K 1999 *Appl. Phys. Lett.* **74** 1939
- [29] Fisher T A, Lidzey D G, Pate M A, Weaver M S, Whittaker D M, Skolnick M S and Bradley D D C 1995 *Appl. Phys. Lett.* **67** 1355
- [30] Jordan R H, Dodabalapur A and Slusher R E 1996 *Appl. Phys. Lett.* **69** 1997